

Cross Reconstruction Transformer for Self-Supervised Time Series Representation Learning

Wenrui Zhang[#], Ling Yang[#], Shijia Geng, Shenda Hong^{*}

Abstract—Unsupervised/self-supervised representation learning in time series is critical since labeled samples are usually scarce in real-world scenarios. Existing approaches mainly leverage the contrastive learning framework, which automatically learns to understand the similar and dissimilar data pairs. Nevertheless, they are restricted to the prior knowledge of constructing pairs, cumbersome sampling policy, and unstable performances when encountering sampling bias. Also, few works have focused on effectively modeling across temporal-spectral relations to extend the capacity of representations. In this paper, we aim at learning representations for time series from a new perspective and propose Cross Reconstruction Transformer (CRT) to solve the aforementioned problems in a unified way. CRT achieves time series representation learning through a cross-domain dropping-reconstruction task. Specifically, we transform time series into the frequency domain and randomly drop certain parts in both time and frequency domains. Dropping can maximally preserve the global context compared to cropping and masking. Then a transformer architecture is utilized to adequately capture the cross-domain correlations between temporal and spectral information through reconstructing data in both domains, which is called Dropped Temporal-Spectral Modeling. To discriminate the representations in global latent space, we propose Instance Discrimination Constraint to reduce the mutual information between different time series and sharpen the decision boundaries. Additionally, we propose a specified curriculum learning strategy to optimize the CRT, which progressively increases the dropping ratio in the training process. We conduct extensive experiments to evaluate the effectiveness of the proposed method on multiple real-world datasets. Results show that CRT consistently achieves the best performance over existing methods by 2%~9%.

Index Terms—Time series, Self supervised learning, Transformer, Cross domain

I. INTRODUCTION

Time series analysis [1] is critical in a variety of real-world applications, such as transportation, medicine, finance, and industry. With the success of deep learning, various tasks in the field of time series analysis have achieved great performances,

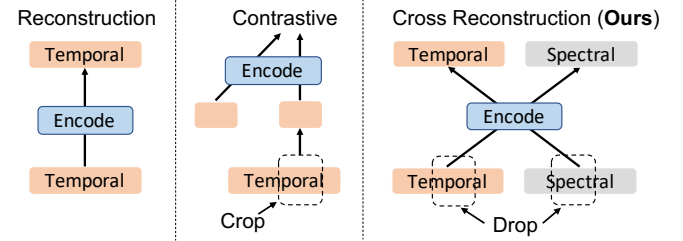


Fig. 1. Comparisons with previous self-supervised methods. “Encode” produces the representations of time series. Note that our CRT utilizes both temporal and spectral information, and captures long-term cross-domain dependencies.

which includes time series classification [2], forecasting [3] and anomaly detection [4]. However, since labeled time series are usually difficult to acquire [5], [6], it is essential to study unsupervised/self-supervised representation learning for time series.

Existing works can be grouped into two categories: reconstruction based and contrast based methods. Reconstruction based methods [7], [8] focus on utilizing the long-term context information for the time series with an encoder-decoder architecture. TimeNet [9] presents a multi-layer RNN sequence-to-sequence autoencoder, while S2S-F-A [10] develops a multi-layer LSTM with an attention mechanism. With the success of transformer architectures [11]–[13], a recent work [14] proposes for the first time a transformer-based framework for unsupervised representation learning of multivariate time series. Contrast based methods [15], [16] are mainly to apply a segment-level sampling policy to conduct the contrastive learning. Contrastive Predictive Coding (CPC) [17] conducts representation learning by using powerful autoregressive models in latent space to make predictions in the future, relying on Noise-Contrastive Estimation [18] for the loss function in similar ways. Temporal and Contextual Contrasting (TS-TCC) [19] is an improved work of CPC and learns robust representations by a harder prediction task against perturbations introduced by different timestamps and augmentations.

We note that existing reconstruction and contrast based methods both have shortcomings: 1) they both fail to exploit the spectral information and neglect to utilize the temporal-spectral correlations in representation learning; 2) segment-level sampling policy used in contrastive learning may cause the sampling bias and it is unable to capture the long-term dependencies.

Wenrui Zhang is with the Department of Mathematics, National University of Singapore, Singapore, 119077, Singapore (e-mail: zhangwenrui@u.nus.edu).

Ling Yang is with the National Institute of Health Data Science, Peking University, and Institute of Medical Technology, Health Science Center of Peking University, Beijing, 100191, China (e-mail: yangling0818@163.com).

Shijia Geng is with the HeartVoice Medical Technology, Hefei, 230027, China (e-mail: gengshijia@heartvoice.com.cn).

Shenda Hong is with the National Institute of Health Data Science, Peking University, and Institute of Medical Technology, Health Science Center of Peking University, Beijing, 100191, China (e-mail: hongshenda@pku.edu.cn).

[#]Equal Contributions.

^{*}Corresponding author.

To solve these problems, we propose Cross Reconstruction Transformer (CRT) for self-supervised time series representation learning. A schematic comparisons are illustrated in Fig. 1. To adequately exploit the spectral information and temporal-spectral correlations, we introduce phase to store more spectral information, and propose the Dropped Temporal-Spectral Modeling. Specifically, we randomly drop certain parts of time series in time and frequency domains, and use the rest as the inputs. We note that dropping can maximally preserve the global context and the original pattern of the time series. Then we apply a transformer encoder to adequately model the cross-domain correlations and acquire expressive representations through reconstructing the original data (including dropped and undropped parts) in both domains. Besides, we devise Instance Discrimination Constraint to reduce the mutual information between different time series for discriminate the representations in global latent space. In addition, we propose a specified curriculum learning strategy to optimize the CRT, which progressively increases the dropping ratio in the pre-training process. We evaluate the representations learned by our proposed method on three datasets, and the results demonstrate that our CRT achieves the best performance in terms of effectiveness and robustness, with a performance gain of 2%~9%.

II. RELATED WORK

Researches on self-supervised representation learning on sequence data have been well-studied [20]–[23], but the representation learning for time series still needs to be promoted. Inspired by the well-studied self-supervised learning methods in computer vision and natural language processing areas [24]–[28], recent works mainly leverage the contrastive learning framework for time series representation learning. The researchers design different time slicing strategies to construct positive and negative pairs with the assumption that temporally similar fragments could be viewed as positive samples and remote fragments are treated as negative samples [29]. Unsupervised Scalable Representation Learning [15] introduces a novel unsupervised loss with time-based negative sampling to train a scalable encoder, shaped as a deep convolutional neural network with dilated convolutions [30]. Temporal Neighborhood Coding [16] introduces the concept of a temporal neighborhood with stationary properties as the distribution of similar windows in time. Nevertheless, these time-based methods are sometimes unreasonable for long time series and fail to capture the long-term dependencies. Besides, they will substantially deteriorate the performance when applied in downstream tasks containing periodic time series.

A recent work [14] firstly proposes a transformer-based reconstruction self-supervised task for time series data. This method masks part of original time series data by setting the values as zeros, and uses a linear layer to reconstruct the masked data. The results show that reconstructing the masked data can help extract dense vector representations of multivariate time series. However, masking original data can cause the gap between the pre-training stage and fine-tuning

stage, because it changes the original distribution of time series significantly. In addition, all methods including contrastive learning methods neglect an important characteristic of time series data - the frequency domain.

III. CROSS RECONSTRUCTION TRANSFORMER

In this section, we will introduce our CRT method in detail. The framework is shown in Figure 2, our CRT is a transformer-based time-frequency domain cross reconstruction method. The goal of our method is to learn representations combining useful information of two domains.

We firstly pay attention to the drawbacks of existing self-supervised learning methods for time series data:

- The existing reconstruction methods for time series mask original data and reconstruct it. However, masking (set to zeros) can significantly change the original pattern of time series and bring many noises to the pre-training process that would deteriorate the performance. To tackle these problem, we propose a new way, dropping to process data in Section III-A.
- Most of representation learning methods for time series neglect frequency domain, which is an complementary perspective to time domain of time series. In Section III-B, we propose a novel way to better utilize the spectral information and model temporal-spectral correlations.

Combining the above two modules, we propose our Dropped Temporal-Spectral Modeling for time series in Section III-C. In Section III-D, we introduce an effective progressive training strategy to improve the stability and capacity of our CRT.

A. Dropping Rather Than Masking

Masking parts of data and reconstructing them is a common paradigm in self-supervised learning tasks especially for natural language processing [31]. Inspired by this, some works mask the original time series by setting the value of certain temporal segments to 0 and reconstructing these segments [14]. However, this may significantly change the original pattern of time series and bring many noises to the representation learning process. Besides, it may cause the gap between the pre-training stage and fine-tuning stage since it lead to the distribution shifts. As shown in Figure 3, masking significantly changes the shape of original time series. Different from images or text, shape is an important and unique pattern for time series [32]. Thus masking would bring noises into the pre-training stage and deteriorate the downstream performance.

In this work, we choose to drop some segments of the time series rather than masking them. Dropping discards the certain parts of input time series, and feeds the rest of the data into the model. The difference between masking and dropping is shown in Figure 3. In detail, we slice the input into patches with the same length, and randomly discard some patches. In this way, the model receives segments of real data without corrupted zeros portions. Thus the model can maximally preserve the global context and capture the intrinsic long-term dependencies.

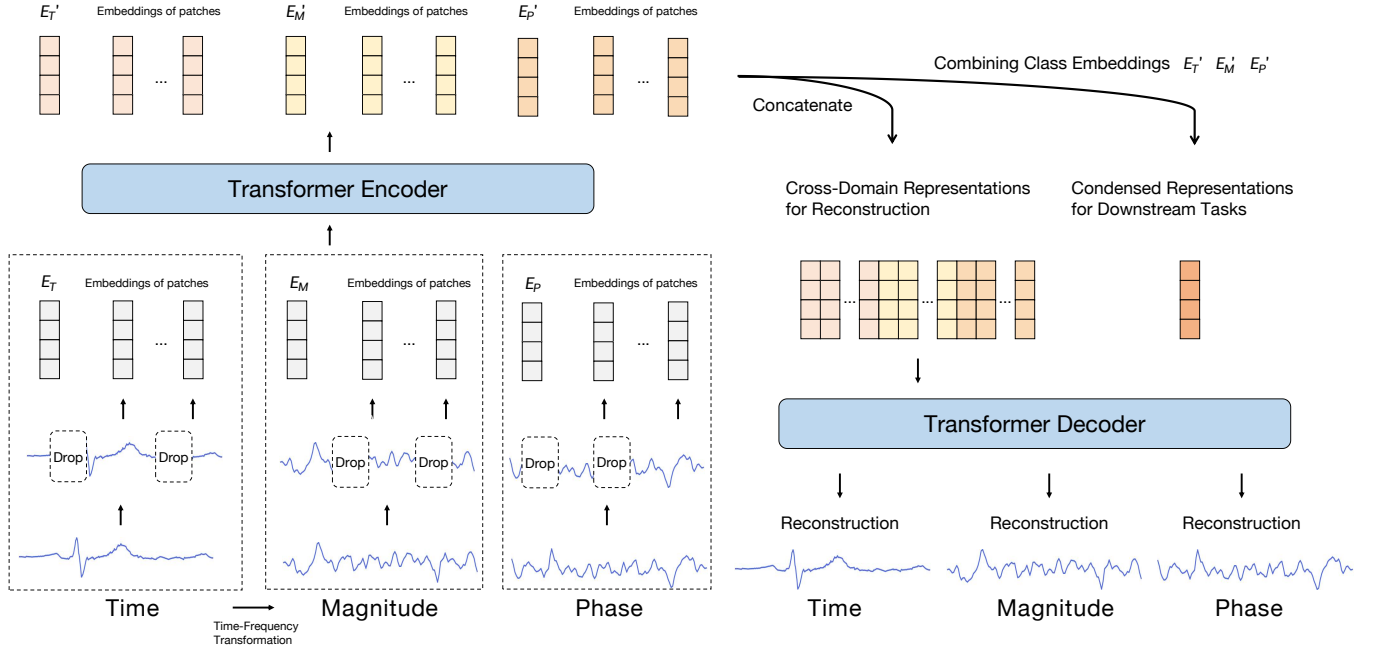


Fig. 2. The framework of our CRT. For each time series, we transform it into the frequency domain and calculate the magnitude and phase as explained in Section III-B. We then slice the data and randomly drop some sliced patches. The remaining patches are projected as three types of embeddings through three convolutional neural networks (not shown in the figure). Decorated with the prefixed [CLS] tokens (E_T , E_M and E_P) and summed with position embedding and domain-type embedding (not shown), all embeddings are fed into a cross-domain transformer encoder. For our pre-trained reconstruction task, we feed all resultant cross-domain representations into the decoder to reconstruct the original time, magnitude and phase data. For downstream tasks, we condense E'_T , E'_M and E'_P (corresponding to E_T , E_M and E_P) as the representation.

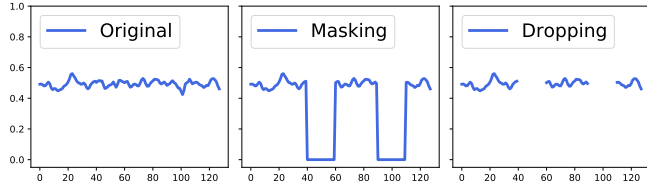


Fig. 3. Masking vs. Dropping. Given one time series data (Top), masking means to set segments of values to zeros (Middle), and dropping means to discard some segments (Bottom).

B. Involving Spectral Information

When learning representations for time series, most of existing methods neglect to involve the spectral information of time series. Frequency domain provides another perspective to discover the patterns for time series data. The spectral perspective can provide several characteristics of the time series that are not acquirable in time domain. Consequently, we attempt to explicitly input both time and frequency domains into model to enable it to learn both temporal and spectral information.

The most common method to transform time series into frequency domain is the Fast Fourier Transform (FFT) [33], which is a rapid implementation of Discrete Fourier Transform (DFT):

$$\mathcal{F}[k] = \sum_{n=0}^{N-1} \mathbf{t}[n] \left(\cos\left(\frac{2\pi kn}{N}\right) - i \sin\left(\frac{2\pi kn}{N}\right) \right) \quad (1)$$

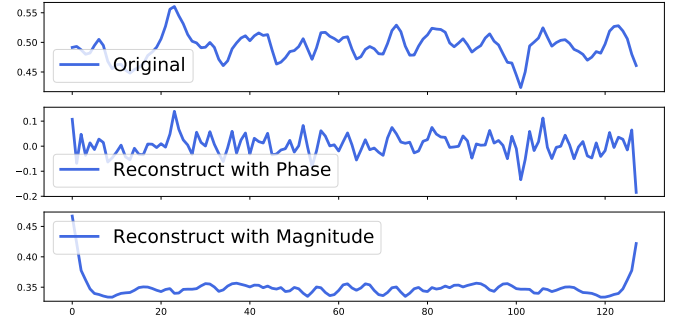


Fig. 4. Phase v.s. Magnitude. Given a time series (Top), reconstruction with phase tends to preserve the shape of the original data (Middle), while reconstruction with magnitude tends to preserve the value of the original data (Bottom).

where \mathbf{t} is original time series data, N is the length of \mathbf{t} , i is called imaginary unit satisfying $i^2 = -1$, and \mathcal{F} is the frequency domain data. After FFT, the original time series is transformed into the frequency domain, and is converted to a sequence of complex numbers. However, these complex numbers cannot be used to train the neural networks directly. Most of the methods considering frequency domain attempt to store the spectral information using the magnitude of the complex numbers. For any complex number $z = a + bi$, where a, b are arbitrary real numbers. The magnitude of z is:

$$||z|| = \sqrt{a^2 + b^2} \quad (2)$$

However, using only magnitude to restore the complex num-

TABLE I
NOTATIONS.

Notation	Definition
\mathbf{t}	The original time series
\mathbf{m}	The magnitude of \mathbf{t}
\mathbf{p}	The phase of \mathbf{t}
\mathbf{x}	Concatenation of \mathbf{t} , \mathbf{m} and \mathbf{p}
r	Dropping ratio
\mathbf{x}_i	The i -th \mathbf{x} in a batch of \mathbf{x}
\mathbf{E}_i	The projection of \mathbf{x}_i by convolutional neural networks
\mathbf{E}'_i	The projection of \mathbf{E}_i by transformer
\mathbf{E}_T	The [CLS] token for time domain
\mathbf{E}'_T	The projection of \mathbf{E}_T by transformer
\mathbf{E}_M	The [CLS] token for magnitude.
\mathbf{E}'_M	The projection of \mathbf{E}_M by transformer
\mathbf{E}_P	The [CLS] token for phase
\mathbf{E}'_P	The projection of \mathbf{E}_P by transformer

bers would cause information loss. Because we can not restore z only using $\|z\|$.

To tackle this problem, we propose a novel way to better utilize the spectral information rather than simply using magnitude. We introduce phase $\phi(z) = \arctan \frac{a}{b}$ which is another characteristic of frequency domain. With phase and magnitude, we can restore the full spectral information which is represented by the complex number z through

$$\begin{aligned} a &= \|z\| \times \sin(\phi(z)), \\ b &= \|z\| \times \cos(\phi(z)), \\ z &= a + bi \end{aligned} \quad (3)$$

In addition to complementing magnitude, phase contains more information relative to the shape of times series. We compare the information contained by phase and magnitude through restoring original time series only using phase or magnitude. In detail, we calculate the phase and magnitude of a time series, and replace phase or magnitude with a constant vector. In both cases, we restore the complex vector following Equation III-B, and conduct inverse FFT to transform complex vectors to time domain. As shown in Figure 4, we can see that the original time series is more similar to the restored time series with correct phase. This intuitively explains why we introduce phase rather than other characteristics of frequency domain.

C. Dropped Temporal-Spectral Modeling

In this section, we will introduce our Dropped Temporal-Spectral Modeling. For a given time series data \mathbf{t} , we firstly conduct FFT on it and convert \mathbf{t} from the time domain to frequency domain. The obtained vector is a complex vector, of which we store both the magnitude and the phase as mentioned in Section III-B. Thus, the complex vector is transformed to two real vectors \mathbf{m} (magnitude) and \mathbf{p} (phase) with the same length. We then concatenate \mathbf{t} , \mathbf{m} , and \mathbf{p} to get the input $\mathbf{x} = [\mathbf{t}, \mathbf{m}, \mathbf{p}]$ of length L .

For the input \mathbf{x} , we choose to drop parts of it as mentioned in Section III-A. Each of the sliced patches contains only one type of data (time, magnitude, or phase). After that,

we drop $r \times N$ ($r \in (0, 1)$ is the given dropping ratio and N is the number of patches) patches and use remained $(1 - r) \times N$ patches to reconstruct the dropped patches. For patches containing time information, we randomly drop them. Also, for patches containing frequency information (phase or magnitude), we drop the corresponding pair of patches (phase and magnitude of the same segments of complex vectors). As explained in Section III-A, dropping the patches can reduce the gap between the pre-training stage and fine-tuning stage because it does not change the shape of the original data.

Before the transformer encoder, we add three convolutional neural networks (CNNs) to extract local features for three types of patches respectively. We think CNN can help extract local features, and transformer can help model cross domain information using the local features. The patches of time, magnitude, and phase are projected to three types of embeddings respectively. Then we add a different learnable [CLS] token before each type of embeddings (\mathbf{E}_T , \mathbf{E}_M and \mathbf{E}_P). The three types of embeddings are summed with their corresponding learnable domain-type embeddings and concatenated into a vector $\mathbf{E} \in \mathbb{R}^{(N+3) \times D}$, where D is the dimension of the embeddings. Before fed into the transformer, \mathbf{E} is summed with the corresponding position embeddings.

We input the whole \mathbf{E} into transformer encoder, and use the produced features to reconstruct original data (time, magnitude and phase). We hope that the learned representations can be used to reconstruct the original two domains' data, so that the transformer encoder can automatically capture complementary information of two domains.

Formally, in a batch, there are B inputs $x_i, i = 1, \dots, B$. \mathbf{x}_i is projected to $\mathbf{E}_i \in \mathbb{R}^{(N+3) \times D}$ by convolutional neural networks, and \mathbf{E}_i is projected by Transformer to $\mathbf{E}'_i \in \mathbb{R}^{(N+3) \times D}$. We use $\bar{\mathbf{E}}'_i = \frac{\mathbf{E}'_T + \mathbf{E}'_M + \mathbf{E}'_P}{3}$ for down-stream tasks. We concatenate each \mathbf{E}'_i with learnable tokens, and feed them into decoder to reconstruct the all patches. The reconstruction loss is:

$$\mathcal{L}_{Recon} = \frac{1}{L \times d} \sum_{i=1}^L \sum_{j=1}^d (x'[i][j] - x[i][j])^2 \quad (4)$$

where x' is the reconstructed input (including both dropped and undropped patches), and d is the dimension of \mathbf{x} .

When reconstructing the original data of two domains, we hope the latent representations contain more sample-specific information and less similar information to other samples. Hence, we propose a simple Instance Discrimination Constraint (IDC) module to remove redundancy and sharpen decision boundary. IDC maximizes the mutual information between the representations and original input, and simultaneously constrain the redundant information that other samples have in common. And we maximize the distance between $\bar{\mathbf{E}}'_i$ and \mathbf{E}_j where $i \neq j$ in latent space, that is minimizing:

$$\mathcal{L}_{IDC} = \frac{1}{B^2} \sum_{i=1}^B \sum_{j=1}^B e^{\text{sim}(\text{Proj}_1(\bar{\mathbf{E}}'_i), \text{Proj}_2(\mathbf{E}_j))} \quad (5)$$

where sim is cosine similarity $\text{sim}(x, y) = \frac{x \cdot y}{\|x\| \|y\|}$, and $\text{Proj}_1, \text{Proj}_2$ are two projection heads to project $\bar{\mathbf{E}}'_i$ and \mathbf{E}_j into the same latent space.

D. Model Optimization

Combining the reconstruction loss and IDC loss, our final loss is:

$$\mathcal{L} = \mathcal{L}_{Recon} + \beta \mathcal{L}_{IDC} \quad (6)$$

where β is a hyper-parameter. By updating this loss, we hope the representations learned by the model contains as much sample-specific information as possible. Thus, the representations is both informative and discriminable.

However, it is difficult to reconstruct the dropped patches when r is initially set as a large value. So we introduce Curriculum Learning (CL) [34], which is a strategy that trains the model from “easy” to “hard”. In detail, we set a relatively small dropping ratio r at the beginning of pre-training stage, and increase r as the self-supervised learning goes. Formally, we refer to the initial r as r_{min} , final r as r_{max} , and the number of epochs for increasing r as N_{epoch} . Then the r for each epoch i is

$$r_i = \max(r_{min}, \min(r_{max}, \frac{i}{N_{epoch}})) \quad (7)$$

When the current epoch i is smaller than $r_{min} \times N_{epoch}$, r_i is equal to r_{min} . When $r_{min} \times N_{epoch} \leq i \leq r_{max} \times N_{epoch}$, r_i is equal to $\frac{i}{N_{epoch}}$. Then, r_i remains r_{max} until the pre-training stage ends.

IV. EXPERIMENTS

A. Experimental Setup

1) *Datasets*: We conduct experiments on three publicly available time series datasets:

- **PTB-XL** [35], [36]. PTB-XL is an electrocardiogram (ECG) dataset with 21,837 12-lead ECGs of 10s, where 52% are male and 48% are female, ranging in age from 0 to 95. The sample rate is 500 Hz, and the length of each recording is 5,000. Our task is to classify time series into one of the five classes including normal ECG (NORM), conduction disturbance (CD), hypertrophy (HYP), myocardial infarction (MI), and ST/T change (STTC).
- **HAR** [37]. HAR is a human activity recognition dataset with 10,299 9-variable time series with a length of 128 from 30 individuals. The data are sampled from the accelerometer and gyroscope with a sampling rate of 50 Hz. Our task is to classify time series into one of the six classes including daily activity, including walking, walking upstairs, downstairs, standing, sitting, and lying down.
- **Sleep-EDF** [36], [38]. Sleep-EDF is built for sleep stage classification. We use data from 4 subjects in their normal daily life recorded by a modified cassette tape recorder. With the sampling rate of 100 Hz, We choose 3 channels: horizontal EOG, FpzCz, and PzOz EEG. Each recording is a 24-hour time series, and we cut them into 30-s segments with a length of 3,000. Our task is to classify time series into one of the eight classes including wake, sleep stage 1, sleep stage 2, sleep stage 3, sleep stage 4, rapid eye movement, movement, and unscored.

The overview of our adopted datasets is shown in Table II.

TABLE II
STATISTICS OF DATASETS.

Dataset	# of samples	# of channels	# of classes	Length
PTB-XL	21,837	12	5	5000
HAR	10,299	9	6	128
Sleep-EDF	22,636	3	8	3000

TABLE III
KEY HYPER-PARAMETERS OF DATASETS.

Dataset	patch size	r_{min}	r_{max}	N_{epoch}
PTB-XL	20	0.3	0.6	200
HAR	8	0.3	0.8	300
Sleep-EDF	20	0.3	0.85	300

All three datasets are randomly split into three parts, training set (80%), validation set (10%), and test set (10%). In real-world scenarios, unlabeled data is much more common than labeled data. To better simulate this situation, we use the whole training set to pre-train, and randomly select 20% of the training set to fine-tune the pre-trained model.

2) *Data processing*: We use `fft` function in `numpy.fft` of Python library. For each channel of a time series data, the original transformed sequence is a complex array with same length. Because of the symmetry of this sequence, we preserve the former half of this sequence, and store the magnitude and phase of this half sequence. After concatenating three sequences, the new sequence is with the double length of original time series. When we slice the sequence into patches, we make sure that each patch contains only one type of data (time, magnitude or phase). And we randomly drop patches in a probability of P_i (as mentioned in Section III-D) in the i -th epoch during pre-training. The patch length and dropping hyper-parameters for each dataset is given in Table III.

3) *Baselines*: We compare our performances with following self-supervised learning approaches, including the ones designed for time series specifically as well as the ones for general data.

- **Contrastive Predictive Coding (CPC)** [17]: CPC is to learn representations by predicting the future data in the latent space through autoregressive models. It constructs a contrastive loss to preserve maximally the mutual information between data in the present time step and data in the future.
- **SimCLR** [28]: SimCLR is a contrastive learning method firstly designed for image data, and it constructs positive pairs and negative pairs by conducting different data augmentation methods. We replace the original encoder architecture with our encoder for a fair comparison. And we use the same augmentations as previous work [39] for time series. The same data with two data augmentation methods form positive pairs, and the other pairs are negative pairs. The self-supervised learning task is to maximize the similarity of positive pairs and minimize the similarity of negative pairs in latent space.
- **Temporal and Contextual Contrasting (TS-TCC)** [19]: TS-TCC is a self-supervised learning method for time

series data. Similar to SimCLR, it transforms the raw time series data into two views by using weak and strong augmentations. The task is a combination of a cross-view prediction task and a contrastive task. The contrastive learning task maximizes the similarity among different views of the same sample while minimizes similarity among views of different samples.

- **Temporal Neighborhood Coding (TNC)** [16]: TNC is also a contrastive learning method for time series data. It utilizes the stationary properties of time series data. Similar to SRL, TNC also constructs positive pairs using near segments, and constructs negative pairs using far segments.
- **Time Series Transformer (TST)** [14]: TST is a self-supervised learning method for time series data by reconstructing the masked parts of original time series data. Different from our method, it neglects the frequency domain and masks the original data by setting the value as 0, which causes a large gap between the pre-training and fine-tuning.

For fair comparisons, we implement these methods using public code with the same encoder architectures as the original work (except SimCLR which is with our encoder architecture). The representation dimensions are all set to 256, the same as ours. All experiments are conducted on a server with 503 GB of RAM and five NVIDIA GeForce RTX 3090ti GPUs.

4) Experiment Settings:

5) *Evaluations*: Linear probing is a popular method to evaluate the self-supervised learning method. However, it restricts the ability of deep learning since it can not pursue stronger and dataset-specific representations. Hence, we add a two-layer fully connected neural network as the classifier after the transformer encoder and fine-tune the whole model. The validation set is used to tune the hyper-parameters (such as β in \mathcal{L} , batch size and learning rate) in fine-tuning stage, and the model reaching the highest accuracy on the validation set is saved and evaluated on the test set.

In self-supervised learning stage, we randomly choose 5 seeds and get 5 pre-trained models. In fine-tuning stage, we also randomly use 5 seeds to fine-tune each of the 5 pre-trained models. Thus, we get 25 results per self-supervised learning method per dataset.

We use ROC-AUC, F1-Score and Accuracy to evaluation the methods. ROC-AUC is defined as the area surrounded by the Receiver Operator Characteristic curve (ROC curve), the x-axis and the y-axis. Regarding ROC curve, it is first computed based on the predicted probability and ground truth of each label directly without a predefined threshold, then defined as the curve of the true positive rate versus the false positive rate at various thresholds ranging from zero to one. Accuracy is calculated for each class, as the ratio of the number of correctly classified samples over the total number of samples. F1 score is the harmonic average of precision (the proportion of true positive cases among the predicted positive cases) and recall (the proportion of positive cases whose are correctly identified). As a multi-class classification task, we report averaged ROC-AUC values across all classes, averaged Accuracy values across all classes, and macro averaged F1 score. We report numbers in percentage values for better reading.

TABLE IV
COMPARISON BETWEEN BASELINE METHODS AND OUR METHOD. THE VALUE BEFORE \pm IS THE MEAN VALUE OF MULTIPLE-TIME RUNS, AND THE VALUE AFTER \pm IS THE STANDARD DEVIATION.

Dataset	Method	ROC-AUC	F1-Score	Accuracy
PTB-XL	CPC	87.42 \pm 0.34	63.17 \pm 1.19	85.75 \pm 0.28
	SimCLR	84.50 \pm 1.45	59.94 \pm 2.49	84.17 \pm 0.80
	TSTCC	87.25 \pm 0.25	65.70 \pm 0.71	84.66 \pm 1.12
	TNC	86.90 \pm 0.35	63.02 \pm 1.13	85.35 \pm 0.23
	TST	81.69 \pm 0.39	59.36 \pm 8.30	81.86 \pm 1.80
	CRT	89.22 \pm 0.07	68.43 \pm 0.58	87.81 \pm 0.29
HAR	CPC	94.83 \pm 1.15	84.42 \pm 2.13	83.86 \pm 2.05
	SimCLR	96.53 \pm 0.88	86.85 \pm 2.26	86.15 \pm 2.37
	TSTCC	97.46 \pm 0.32	88.68 \pm 1.43	87.95 \pm 1.59
	TNC	94.45 \pm 1.32	84.64 \pm 1.96	84.01 \pm 1.95
	TST	97.31 \pm 0.39	86.17 \pm 1.00	85.37 \pm 1.01
	CRT	98.94 \pm 0.22	90.51 \pm 0.77	90.09 \pm 0.75
Sleep-EDF	CPC	91.92 \pm 1.62	39.74 \pm 3.35	88.70 \pm 1.35
	SimCLR	91.97 \pm 3.22	41.78 \pm 3.13	87.86 \pm 1.77
	TSTCC	93.57 \pm 1.83	39.09 \pm 4.50	86.06 \pm 3.19
	TNC	91.48 \pm 3.51	37.89 \pm 5.13	86.97 \pm 3.48
	TST	93.31 \pm 2.29	42.58 \pm 2.48	88.83 \pm 0.84
	CRT	94.74 \pm 1.09	44.38 \pm 1.14	90.12 \pm 0.57

B. Comparison Results

We compare our CRT with baseline methods and show the results in Table IV. Our CRT outperforms all baselines in terms of ROC-AUC, F1-score and accuracy. We also observe that results of CRT have relatively small standard deviation, which implies a more stable performance on down-stream tasks. In addition, we notice that TST (another reconstruction-based self-supervised learning method) also obtains a relatively small standard deviation. The reason might be that reconstruction tasks do not require constructing negative and positive pairs, which is difficult and may cause instability. It indicates that reconstruction-based methods may provide a more stable way for self-supervised learning. One baseline named Scalable Representation Learning [15] is not included in our results, as it requires much longer running time and we failed to produce its results in several days.

C. Analysis of Cross-Domain Reconstruction

More ablation studies and comparison experiments are conducted to further verify the effectiveness of our method.

1) *Dropping is Better than Masking*: To verify that dropping can better alleviate the gap between pre-training and fine-tuning than masking, we compare the results on down-stream tasks under the two setups. From Figure 5, we see dropping always leads to better down-stream performances, except for the Sleep-EDF dataset, where dropping yields a slightly lower ROC-AUC but outperforms masking for other metrics. This is because zeros brought by masking may create wrong patterns for time series data, and dropping can tackle this problem. Our dropping can keep the shape of the original time series, and reduce the gap between pre-training and fine-tuning caused by masking.

2) *Adding Phase Helps Frequency Learning*: We also conduct a simple ablation study to support that phase can provide supplementary spectral information. We evaluate the model pre-trained and fine-tuned with and without phase data under

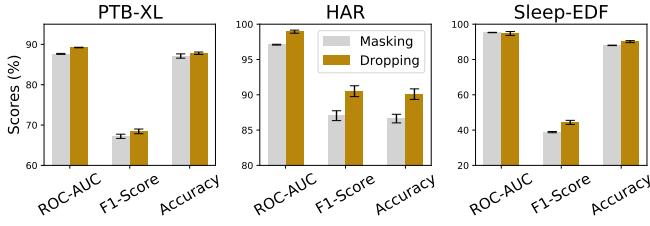


Fig. 5. The performance on three datasets when data is dropped or masked during pre-training stage.

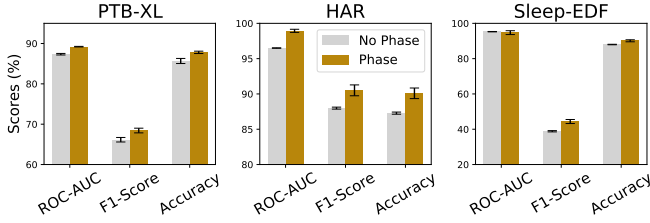


Fig. 6. The performance on three datasets with and without phase.

the same experimental setups as our CRT. The results on three datasets with and without phase data are shown in Figure 6. We can see that adding phase can help improve the final performance in terms of three metrics. This supports our view that magnitude is not informative enough to represent the frequency domain, and phase can complement magnitude.

3) *Cross-Domain is Better than Single-Domain*: We compare our method with the trivial single-domain reconstruction tasks. After conducting time-domain and frequency-domain (phase and magnitude) reconstruction tasks respectively, we fine-tune the models using the corresponding domain’s data. As shown in Table VI, CRT performs best in terms of all 3 metrics. The ROC-AUCs of all 5 classes on PTB-XL datasets are shown in the left in Figure 7. We can see that cross-domain representations help improve performance on all classes. This is because some abnormalities of ECGs can be more easily observed from the perspective of frequency domain. The right figure of Figure 7 shows the performance on Sleep-EDF dataset under different training size. We give the results when 20%, 40%, 60% and 80% of training set is used for finetuning. The results show that combining two domains,

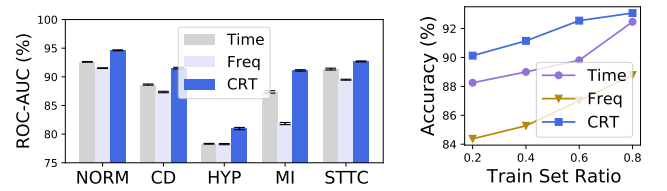


Fig. 7. The performance when using time domain, frequency domain and both domains. **Left**: ROC-AUC of all 5 classes on PTB-XL. **Right**: Accuracy on Sleep-EDF when the ratio of training set used for fine-tuning is 0.2, 0.4, 0.6 and 0.8.

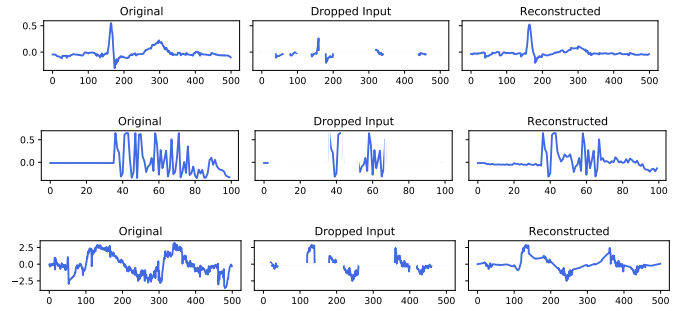


Fig. 8. Three reconstructed cases (the “Reconstructed” row) from PTB-XL (top), HAR (middle) and Sleep-EDF (bottom). “Original” represents the original time series, and “Dropped input” represents time series after being dropped.

our cross domain representations can yield higher accuracy under different ratios.

All results support our hypothesis that learning from two domains can yield more informative representations than from single domain. This is because some patterns of frequency domain can complement the temporal patterns. Also, the cross domain transformer encoder can fuse different types of features, and extract useful and complementary patterns from two domains.

In addition, we also notice that in all three datasets, using time domain yields better performance compared with using frequency domain. This may because the patterns of time domain are more direct for neural networks to discover, and the three classification tasks are strongly related to these patterns. However, adding frequency domain can supplement some patterns, leading to better performance.

TABLE V

THE COMPARISON OF CROSS-DOMAIN AND SINGLE-DOMAIN. TIME REPRESENTS TIME-TO-TIME RECONSTRUCTION AND FREQ REPRESENTS FREQUENCY-TO-FREQUENCY RECONSTRUCTION.

Dataset	Method	ROC-AUC	F1-Score	Accuracy
PTB-XL	Time	88.08 \pm 0.25	67.45 \pm 0.55	85.67 \pm 0.59
	Freq	77.58 \pm 0.43	47.86 \pm 1.96	78.28 \pm 0.91
	CRT	89.22 \pm 0.07	68.43 \pm 0.58	87.81 \pm 0.29
HAR	Time	96.46 \pm 0.13	87.62 \pm 1.00	86.84 \pm 1.07
	Freq	94.61 \pm 0.14	76.96 \pm 1.38	76.50 \pm 1.44
	CRT	98.94 \pm 0.22	90.51 \pm 0.77	90.09 \pm 0.75
Sleep-EDF	Time	94.64 \pm 0.55	40.13 \pm 1.30	88.25 \pm 0.59
	Freq	91.00 \pm 0.76	38.07 \pm 1.88	84.37 \pm 1.33
	CRT	94.74 \pm 1.09	44.38 \pm 1.14	90.12 \pm 0.57

TABLE VI

COMPARISONS OF THREE KINDS OF CROSS-DOMAIN RECONSTRUCTION. T2F REPRESENTS TIME-TO-FREQUENCY AND F2T REPRESENTS FREQUENCY-TO-TIME.

Dataset	Method	ROC-AUC	F1-Score	Accuracy
PTB-XL	T2F	84.14 \pm 0.34	59.02 \pm 2.04	83.58 \pm 0.78
	F2T	83.72 \pm 0.49	59.19 \pm 1.95	83.42 \pm 0.70
	CRT	89.22 \pm 0.07	68.43 \pm 0.58	87.81 \pm 0.29
HAR	T2F	98.18 \pm 0.58	89.23 \pm 1.64	88.84 \pm 1.70
	F2T	97.93 \pm 0.83	88.90 \pm 1.97	88.53 \pm 1.98
	CRT	98.94 \pm 0.22	90.51 \pm 0.77	90.09 \pm 0.75
Sleep-EDF	T2F	94.36 \pm 1.66	40.41 \pm 3.65	89.09 \pm 2.62
	F2T	92.88 \pm 1.53	41.67 \pm 1.93	89.46 \pm 1.00
	CRT	94.74 \pm 1.09	44.38 \pm 1.14	90.12 \pm 0.57

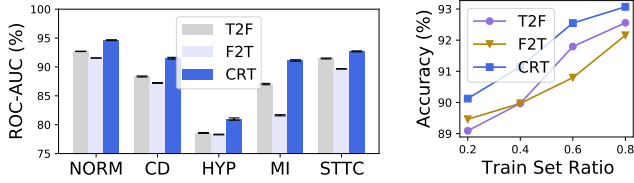


Fig. 9. The performance of three cross-domain reconstruction methods. **Left:** ROC-AUC of all 5 classes on PTB-XL. **Right:** Accuracy on Sleep-EDF when the ratio of training set used for fine-tuning is 0.2, 0.4, 0.6 and 0.8.

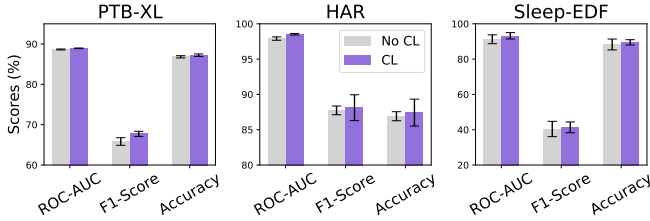


Fig. 10. The performance on three datasets with and without CL.

4) *Exploring Cross-Domain Learning:* We explore the cross-domain learning with two experiments:

- **Time-to-Frequency Reconstruction (T2F):** with only the time-domain part of \mathbf{E} fed into the transformer encoder, we use the encoded features to reconstruct the dropped original frequency-domain data (including phase and magnitude).
- **Frequency-to-Time Reconstruction (F2T):** contrary to T2F, we input the frequency-domain part of \mathbf{E} and reconstruct the dropped time-domain data.

In fine-tuning stage, the input is same as our CRT, to only evaluate the cross reconstruction tasks.

As shown in Table VI, our complete cross-domain solution outperforms the other two methods on three datasets. We also give the results of all 5 classes on PTB-XL dataset (Figure 9 left), and the accuracy on Sleep-EDF dataset under 4 training set ratios (Figure 9 right). From the left figure, we can see CRT outperforms others on all classes, especially on “MI” (11.6% higher than F2T and 4.7% higher than T2F). In the right figure, CRT also performs better, and T2F performs similarly to F2T.

Our CRT adopts transformer as part of our encoder to fuse the embeddings from different domains. The representations obtained from the transformer encoder contain information of both time domain and frequency domain, which benefits the reconstruction as well as the down-stream tasks. Compared with CRT, T2F and F2T only capture a single-direction relationship rather than the mutual relationship. It is intuitive that CRT can produce more semantic representations, and the experiment results well prove it.

5) *CL and IDC Help Learning Cross-Domain Representations:* We conduct another ablation study to verify the effectiveness of CL and IDC, and show the results in Figure 10 and Figure 11.

As we expect, these two modules facilitate learning cross-domain representations. CL helps the reconstruction tasks, and improves the performance on down-stream tasks. We think CL can help better reconstruct the original data, because it gives

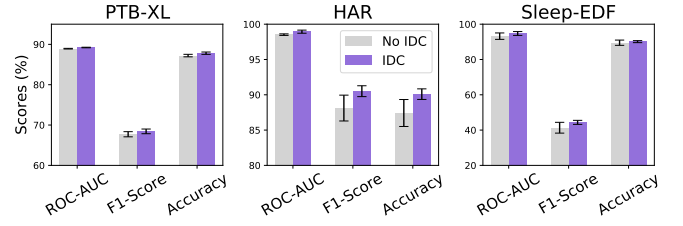


Fig. 11. The performance on three datasets with and without IDC.

a progressively increasing dropping ratio rather a constant large dropping ratio. As a regularization, IDC minimizes the mutual information between different samples which helps transformer extracts more discriminable patterns. It is worth noting that IDC is not a contrastive loss, since it does not minimize distance of any pair of samples. It is only to minimize common information of all time series.

In Figure 8, we illustrate three reconstructed cases with the dropping ratio as 0.7. We can see that the model could almost reconstruct the trend of dropped inputs with such a high dropping ratio, especially for the ECG case from the PTB-XL dataset. The reason for the well-performed ECG reconstruction might be because that ECG is periodic and there are abundant similar patterns in the time series. Such amazing reconstruction performance also proves that our cross-domain representations are highly informative and sample-specific.

V. CONCLUSION

In this work, we propose Cross Reconstruction Transformer (CRT), a cross-domain reconstruction framework based on transformer for self-supervised representations learning of time series data. We note that the existing self-supervised learning methods neglect to utilize the spectral information and temporal-spectral correlations of time series. Moreover, existing “masking” based method for reconstruction tasks tend to significantly change the original pattern of time series, which would lead to the distribution shifts between pre-training and fine-tuning processes. To tackle these problems in a unified way, we propose our cross-domain reconstruction framework which outperforms existing methods on three widely-used datasets. In addition, we conduct various experiments to verify the effectiveness of each component of our framework. For future work, we would adapt our framework to the out-of-distribution scenarios and address more challenging problems.

ACKNOWLEDGEMENT

This work was supported by the National Natural Science Foundation of China (No.62102008).

REFERENCES

- [1] B. N. Oreshkin, D. Carpio, N. Chapados, and Y. Bengio, “N-beats: Neural basis expansion analysis for interpretable time series forecasting,” in *International Conference on Learning Representations*, 2020.
- [2] P. Esling and C. Agon, “Time-series data mining,” *ACM Computing Surveys (CSUR)*, vol. 45, no. 1, pp. 1–34, 2012.
- [3] C. Deb, F. Zhang, J. Yang, S. E. Lee, and K. W. Shah, “A review on time series forecasting techniques for building energy consumption,” *Renewable and Sustainable Energy Reviews*, vol. 74, pp. 902–924, 2017.

- [4] N. Laptev, S. Amizadeh, and I. Flint, “Generic and scalable framework for automated time-series anomaly detection,” in *Proceedings of the 21th ACM SIGKDD International Conference on Knowledge Discovery and Data Mining*, New York, NY, USA, 2015, p. 1939–1947.
- [5] A. Hyvarinen and H. Morioka, “Unsupervised feature extraction by time-contrastive learning and nonlinear ica,” *Advances in Neural Information Processing Systems*, vol. 29, 2016.
- [6] X. Lan, D. Ng, S. Hong, and M. Feng, “Intra-inter subject self-supervised learning for multivariate cardiac signals,” *arXiv preprint arXiv:2109.08908*, 2021.
- [7] F. M. Bianchi, L. Livi, K. Ø. Mikalsen, M. Kampffmeyer, and R. Jenssen, “Learning representations of multivariate time series with missing data,” *Pattern Recognition*, vol. 96, p. 106973, 2019.
- [8] C. Zhang, D. Song, Y. Chen, X. Feng, C. Lumezanu, W. Cheng, J. Ni, B. Zong, H. Chen, and N. V. Chawla, “A deep neural network for unsupervised anomaly detection and diagnosis in multivariate time series data,” in *Proceedings of the AAAI conference on artificial intelligence*, vol. 33, no. 01, 2019, pp. 1409–1416.
- [9] P. Malhotra, V. TV, L. Vig, P. Agarwal, and G. Shroff, “Timenet: Pre-trained deep recurrent neural network for time series classification,” *arXiv preprint arXiv:1706.08838*, 2017.
- [10] X. Lyu, M. Hueser, S. L. Hyland, G. Zerveas, and G. Raetsch, “Improving clinical predictions through unsupervised time series representation learning,” *arXiv preprint arXiv:1812.00490*, 2018.
- [11] A. Vaswani, N. Shazeer, N. Parmar, J. Uszkoreit, L. Jones, A. N. Gomez, L. Kaiser, and I. Polosukhin, “Attention is all you need,” in *Advances in neural information processing systems*, 2017, pp. 5998–6008.
- [12] A. Dosovitskiy, L. Beyer, A. Kolesnikov, D. Weissenborn, X. Zhai, T. Unterthiner, M. Dehghani, M. Minderer, G. Heigold, S. Gelly *et al.*, “An image is worth 16x16 words: Transformers for image recognition at scale,” *arXiv preprint arXiv:2010.11929*, 2020.
- [13] H. Zhou, S. Zhang, J. Peng, S. Zhang, J. Li, H. Xiong, and W. Zhang, “Informer: Beyond efficient transformer for long sequence time-series forecasting,” in *Proceedings of AAAI*, 2021.
- [14] G. Zerveas, S. Jayaraman, D. Patel, A. Bhamidipaty, and C. Eickhoff, “A transformer-based framework for multivariate time series representation learning,” in *Proceedings of the 27th ACM SIGKDD Conference on Knowledge Discovery & Data Mining*, 2021, pp. 2114–2124.
- [15] J.-Y. Franceschi, A. Dieuleveut, and M. Jaggi, “Unsupervised scalable representation learning for multivariate time series,” *Advances in neural information processing systems*, vol. 32, 2019.
- [16] S. Tonekaboni, D. Eytan, and A. Goldenberg, “Unsupervised representation learning for time series with temporal neighborhood coding,” *arXiv preprint arXiv:2106.00750*, 2021.
- [17] A. v. d. Oord, Y. Li, and O. Vinyals, “Representation learning with contrastive predictive coding,” *arXiv preprint arXiv:1807.03748*, 2018.
- [18] M. Gutmann and A. Hyvärinen, “Noise-contrastive estimation: A new estimation principle for unnormalized statistical models,” in *Proceedings of the Thirteenth International Conference on Artificial Intelligence and Statistics*, ser. Proceedings of Machine Learning Research, Y. W. Teh and M. Titterton, Eds., vol. 9, Chia Laguna Resort, Sardinia, Italy, 13–15 May 2010, pp. 297–304.
- [19] E. Eldele, M. Ragab, Z. Chen, M. Wu, C. K. Kwok, X. Li, and C. Guan, “Time-series representation learning via temporal and contextual contrasting,” in *Proceedings of the Thirtieth International Joint Conference on Artificial Intelligence, IJCAI-21*, Z.-H. Zhou, Ed. International Joint Conferences on Artificial Intelligence Organization, 8 2021, pp. 2352–2359.
- [20] J. Chung, K. Kastner, L. Dinh, K. Goel, A. C. Courville, and Y. Bengio, “A recurrent latent variable model for sequential data,” *Advances in neural information processing systems*, vol. 28, pp. 2980–2988, 2015.
- [21] M. Fraccaro, S. K. Sønderby, U. Paquet, and O. Winther, “Sequential neural models with stochastic layers,” *Advances in neural information processing systems*, vol. 29, 2016.
- [22] R. G. Krishnan, U. Shalit, and D. Sontag, “Structured inference networks for nonlinear state space models,” in *Proceedings of the Thirty-First AAAI Conference on Artificial Intelligence*, 2017, pp. 2101–2109.
- [23] J. Bayer, M. Soelch, A. Mirchev, B. Kayalibay, and P. van der Smagt, “Mind the gap when conditioning amortised inference in sequential latent-variable models,” *arXiv preprint arXiv:2101.07046*, 2021.
- [24] E. L. Denton *et al.*, “Unsupervised learning of disentangled representations from video,” *Advances in neural information processing systems*, vol. 30, 2017.
- [25] M. U. Gutmann and A. Hyvärinen, “Noise-contrastive estimation of unnormalized statistical models, with applications to natural image statistics,” *Journal of Machine Learning Research*, vol. 13, no. 2, 2012.
- [26] X. Wang and A. Gupta, “Unsupervised learning of visual representations using videos,” in *Proceedings of the IEEE international conference on computer vision*, 2015, pp. 2794–2802.
- [27] M. Pagliardini, P. Gupta, and M. Jaggi, “Unsupervised learning of sentence embeddings using compositional n-gram features,” in *Proceedings of the 2018 Conference of the North American Chapter of the Association for Computational Linguistics: Human Language Technologies, Volume 1 (Long Papers)*, 2018, pp. 528–540.
- [28] T. Chen, S. Kornblith, M. Norouzi, and G. Hinton, “A simple framework for contrastive learning of visual representations,” in *Proceedings of the 37th International Conference on Machine Learning*, ser. Proceedings of Machine Learning Research, vol. 119, 13–18 Jul 2020, pp. 1597–1607.
- [29] Z. Yue, Y. Wang, J. Duan, T. Yang, C. Huang, Y. Tong, and B. Xu, “Ts2vec: Towards universal representation of time series,” *arXiv preprint arXiv:2106.10466*, 2021.
- [30] A. Van Den Oord, S. Dieleman, H. Zen, K. Simonyan, O. Vinyals, A. Graves, N. Kalchbrenner, A. W. Senior, and K. Kavukcuoglu, “Wavenet: A generative model for raw audio,” *SSW*, vol. 125, p. 2, 2016.
- [31] J. Devlin, M.-W. Chang, K. Lee, and K. Toutanova, “Bert: Pre-training of deep bidirectional transformers for language understanding,” *arXiv preprint arXiv:1810.04805*, 2018.
- [32] L. Ye and E. Keogh, “Time series shapelets: a new primitive for data mining,” in *Proceedings of the 15th ACM SIGKDD international conference on Knowledge discovery and data mining*, 2009, pp. 947–956.
- [33] A. V. Oppenheim, A. S. Willsky, and S. H. Nawab, *Signals & Systems (2Nd Ed.)*. Prentice-Hall, Inc., 1996.
- [34] Y. Bengio, J. Louradour, R. Collobert, and J. Weston, “Curriculum learning,” in *Proceedings of the 26th annual international conference on machine learning*, 2009, pp. 41–48.
- [35] P. Wagner, N. Strodthoff, R.-D. Boussejot, D. Kreiseler, F. I. Lunze, W. Samek, and T. Schaeffter, “Ptb-xl, a large publicly available electrocardiography dataset,” *Scientific data*, vol. 7, no. 1, pp. 1–15, 2020.
- [36] A. L. Goldberger, L. A. Amaral, L. Glass, J. M. Hausdorff, P. C. Ivanov, R. G. Mark, J. E. Mietus, G. B. Moody, C.-K. Peng, and H. E. Stanley, “Physiobank, physiotoolkit, and physionet: components of a new research resource for complex physiologic signals,” *circulation*, vol. 101, no. 23, pp. e215–e220, 2000.
- [37] D. Anguita, A. Ghio, L. Oneto, X. Parra Perez, and J. L. Reyes Ortiz, “A public domain dataset for human activity recognition using smartphones,” in *Proceedings of the 21th international European symposium on artificial neural networks, computational intelligence and machine learning*, 2013, pp. 437–442.
- [38] B. Kemp, A. H. Zwinderman, B. Tuk, H. A. Kamphuisen, and J. J. Obery, “Analysis of a sleep-dependent neuronal feedback loop: the slow-wave microcontinuity of the eeg,” *IEEE Transactions on Biomedical Engineering*, vol. 47, no. 9, pp. 1185–1194, 2000.
- [39] E. Eldele, Z. Chen, C. Liu, M. Wu, C.-K. Kwok, X. Li, and C. Guan, “An attention-based deep learning approach for sleep stage classification with single-channel eeg,” *IEEE Transactions on Neural Systems and Rehabilitation Engineering*, vol. 29, pp. 809–818, 2021.